Hindawi Publishing Corporation
Journal of Nanoscience
Volume 2015, Article ID 362023, 9 pages
http://dx.doi.org/10.1155/2015/362023

Research Article

A Simple and Facile Solvothermal Synthesis of Hierarchical PbS Microstars with Multidendritic Arms and Their Optical Properties

Yong-Fang Li,[1] Ming Zhang,[2] Qi-Jing Yang,[3] Feng-Xian Zhang,[3] Mei-Qi Zheng,[3] and Ai-Jun Wang[3]

[1]*College of Chemistry and Chemical Engineering, Henan Institute of Science and Technology, Xinxiang 453003, China*
[2]*School of Chemistry and Chemical Engineering, Henan Normal University, Xinxiang 453007, China*
[3]*College of Geography and Environmental Science, Zhejiang Normal University, Jinhua 321004, China*

Correspondence should be addressed to Ai-Jun Wang; ajwang@zjnu.cn

Received 3 October 2014; Revised 31 January 2015; Accepted 31 January 2015

Academic Editor: Oleg Lupan

A simple and facile approach was developed in the solvothermal synthesis of hierarchical PbS microstars with multidendritic arms, which were characterized by X-ray diffraction (XRD), scanning electron microscopy (SEM), transmission electron microscopy (TEM), Fourier transform infrared (FT-IR) and photoluminescence (PL) spectroscopy. The morphologies of PbS products were strongly determined by the reaction time and temperature, the ratios of the precursors, and the mixed solvent with various components, and thereby their possible formation mechanism was discussed in some detail. The as-prepared PbS crystals displayed a sharp and strong photoluminescent peak at 437 nm at room temperature. It has potential and practical applications in photoluminescence, photovoltaics, IR photodetectors, electroluminescence, and solar absorbers.

1. Introduction

The intrinsic properties of nanomaterials are strongly determined by their chemical composition, crystallinity, particle size, and morphologies [1, 2]. Recently, semiconductor nanostructures have attracted considerable interest because of their widespread applications in light emitting diodes, microelectronics, light energy conversion, nonlinear optics, biological fluorescence labeling, and photocatalysis [3–5]. For example, Jin and coworkers fabricated self-reporting ZnO tetrapod/elastomer composites which could change luminescent properties under deformation [6]. Lupan et al. synthesized highly crystalline α-MoO_3 nano- and microbelts and ribbons, which were integrated into the chip in the form of nanodevices [7]. Mishra et al. fabricated macroscopically flexible and highly porous hierarchical semiconductor networks for diverse technological applications [8]. Reimer et al. investigated ZnO nano- and microneedles directly integrated in Si trenches on wafer as advanced photocatalytic and optical materials [9].

As one of the semiconductors, PbS is important because of its large excitation, Bohr radius of 18 nm, narrow band gap of 0.41 eV in the bulk form, and diverse morphologies [3, 4, 10–12]. PbS nanostructures have a strong quantum size effect [10, 13], which are widely used in optical switches, flame monitors, near-infrared photodetectors, sensors, lasers, and thermal and biological images [2, 12, 14–18]. Many efforts have been devoted to the control synthesis of PbS nanostructures with various shapes [10], such as spheres, cubes, tubes, wires, dendrites, flowers, and complex hierarchical stars [3, 11, 16, 19–23]. Among them, complex hierarchical PbS stars attract considerable attention and are widely used in many fields [4, 12, 24, 25].

Up to now, many methods have been developed, including colloidal solutions, solvothermal synthesis, microwave irradiation and decomposition, self-assembly, thermolysis, chemical vapor deposition, surfactant, and polymer assisted template method [3, 23, 25–27]. For example, PbS nanocrystals with variable sizes and shapes were fabricated through the thermolysis of the metal complex with sulfur at high

temperature [1, 28, 29]. Recently, star-like and dendritic PbS nanocrystals were constructed by using surfactant-assisted hydrothermal methods [1, 4, 24], microwave irradiation [1, 4, 30], and thermal decomposition [1, 4, 24, 31]. Lately, hierarchical PbS microstars with octa-symmetric-dendritic arms were prepared under hydrothermal conditions [16]. Among them, strong matrix supports are usually required to steady the newly generated nano- and micromaterials, including polymers, zeolites, inverse micelles, and monolayer surfaces [10, 30, 32], where the release of hydrogen sulfide (H_2S) is inevitable. Furthermore, it is still a challenge to develop a simple, environmentally friendly, and universal technique for large-scale synthesis of ordered hierarchical PbS nanocrystals.

It is known that diphenylthiocarbazone contains =S, –NH, –N–N–, –N=N–, and benzene ring, while only =S can serve as the sulfur source and interact with inorganic cations such as lead ions (Pb^{2+}) to form the precursor complexes. Therefore, a simple and facile solvothermal method was developed in the synthesis of hierarchical PbS microstars with multidendritic arms, effectively preventing the emission of H_2S in the present system. Meanwhile, the growth mechanism of hierarchical PbS microstars was also discussed in some detail.

2. Experimental Section

2.1. Chemicals. Diphenylthiocarbazone ($C_{13}H_{12}N_4S$), $Pb(CH_3COO)_2{\cdot}3H_2O$, ethylenediamine (EDA), and ethanol were all obtained from Aladdin Chemistry Co. Ltd (Shanghai, China). All the other chemicals were of analytical grade and used as received without further purification. All the aqueous solutions were prepared with twice-distilled water in the whole experiments.

2.2. Synthesis. Typical experiments are described as follows: 0.379 g (1 mmol) of lead acetate ($Pb(CH_3COO)_2{\cdot}3H_2O$) and 0.256 g (1 mmol) of diphenylthiocarbazone ($C_{13}H_{12}N_4S$) were put into 15 mL of ethylenediamine (EDA) solutions under stirring, respectively. Then, the two solutions were mixed together under stirring. The resultant mixture was transferred into a 50 mL Teflon-lined stainless steel autoclave, sealed, maintained at 180°C for 2 h, and then cooled to room temperature naturally. The precipitates were collected, completely washed with ethanol and water, respectively, and dried in vacuum at 60°C.

Controlled experiments were performed by varying the volume ratios of EDA to water, the volume ratios of EDA to ethanol (EA), the amount of diphenylthiocarbazone, and the reaction time or temperature, while other conditions were kept constant.

2.3. Characterization. The products were characterized by X-ray diffraction (XRD) with a Bruker-D8-AXS diffractometer equipped with a Cu Ka source. SEM images of the samples were obtained with a JEOL-JSM-6390 LV field emission scanning electron microscope. Transmission electron microscopy (TEM) and high-resolution transmission electron microscopy (HRTEM) images were taken with a JEOL JEM-2100F system at 200 kV accelerating voltage. Fourier transform infrared (FT-IR) spectra were obtained by using a MAGNA-IR-750. Photoluminescence (PL) spectrum measured on a Hitachi FP-6500 fluorescence spectrophotometer.

3. Results and Discussion

3.1. Characterization of PbS Microstars. The morphologies of the typical product were characterized by SEM and TEM images (Figure 1). The low- and high-magnification SEM images reveal that the products are composed of many well-defined hierarchical PbS microstars with different numbers of symmetric-dendritic arms as subunits (Figures 1(a) and 1(b)). Each dendritic arm includes a long primary backbone with a length of 3.5 μm, which extends radically from the center. The secondary branches possess hierarchical structures, including two groups of layered and symmetrical PbS lobules with the thickness of 200 nm and the length from 100 to 500 nm (inset in Figure 1(b)). The width of the lobules is in the range of 150–400 nm. Their length (up to 500 nm) and width (up to 400 nm) are varied at different position of the arm, as also confirmed by the TEM image of a single dendritic arm (Figure 1(c)). Meanwhile, HRTEM measurements confirm high crystallinity of PbS microstars (Figure 1(d)), where distinct and successive lattice fringes are observed with the distance of 0.292 nm that is in good agreement with the (200) lattice spacing of PbS [2, 19, 21]. Single crystallinity of PbS microstars is further verified by the corresponding selected area electron diffraction (SAED) pattern marked with different positions (inset in Figure 1(d)) [2, 24, 25].

As displayed in Figure 2(a), the representative diffraction peaks of PbS product in the XRD spectra are matched well with the galena structure of PbS (JCPDS no. 05-0592). The strong and sharp peaks reveal that the as-prepared products are highly crystalline. And the intensity of the (200) peak is much stronger than that of the (111) peak, indicating a higher growth rate on the (100) planes as compared to the (111) planes [3].

In the FT-IR spectrum of diphenylthiocarbazone (Figure 2(b), curve a), the absorption peaks at 3445, 2962, 1594 and 1499, 1438, 1221, 1145, 888, 679, and 752 cm^{-1} correspond to the stretching vibration mode of N–H band, methylene C–H asymmetric vibration band, benzene ring stretching band, C=S stretching mode, deformation vibration of N–H band, C–H inplane bending vibration of benzene ring, N–N stretching mode, and benzene ring deformation vibration mode, respectively [33]. As shown in Figure 2(b) (curves b–g), the peaks belonging to diphenylthiocarbazone disappeare, only leaving one strong broad peak at 3451 cm^{-1} corresponding to the O–H stretching vibration of water [34]. The result demonstrates that the Pb^{2+}-diphenylthiocarbazone complexes are formed and then gradually thermal-decomposed to PbS during the solvothermal process.

Interestingly, control experiments regarding the time-dependent experiments reveal that the reaction time has critical effects on the morphology of the final products (Figure 3), where the morphologies are transformed from immature single dendritic arm (0.5 h, Figure 3(a)) to immature (1 h,

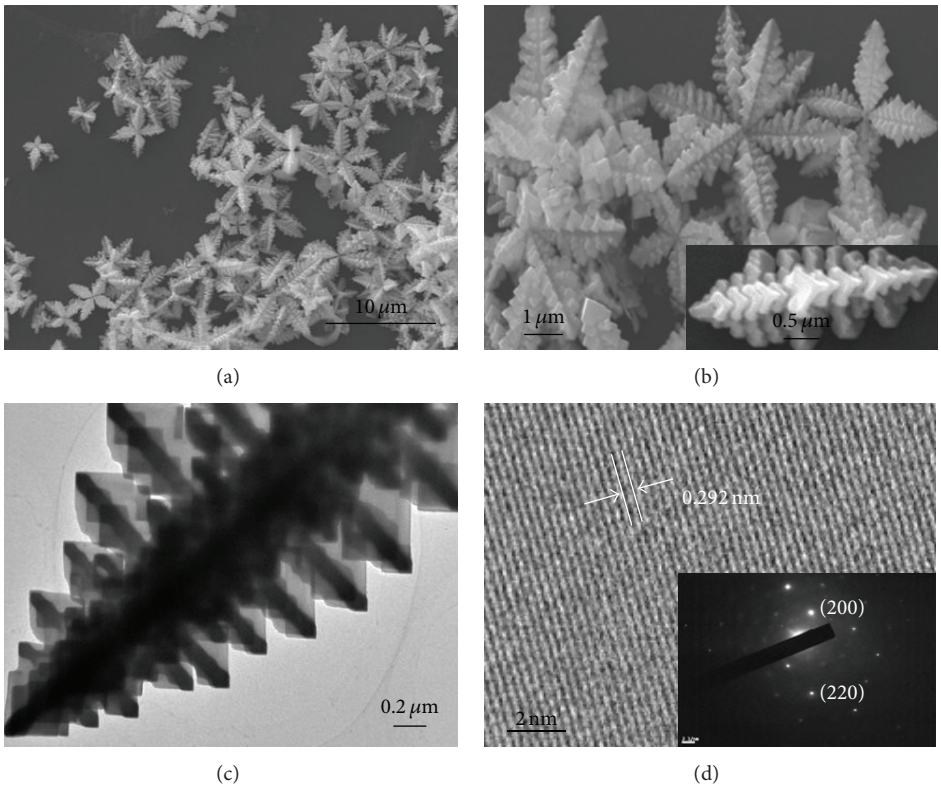

Figure 1: Low- (a) and high-magnification (b) SEM images, TEM (c), and HRTEM (d) images of hierarchical PbS microstars with multidendritic arms. Inset in (b) shows the SEM image of a single dendritic arm. Inset in (d) displays the corresponding SAED pattern.

Figure 3(b)) and well-defined hierarchical microstars (2 h, Figure 1) when the reaction time is below 2 h. Nevertheless, many single dendritic arms are composed of rod-like structures instead of the lobules as building blocks (8 h, Figure 3(c)), as well as the complete disappearance of the lobules-assembled single dendrites (16 h, Figure 3(d)). However, the reaction time nearly has no obvious effects on the purity and phase of the final products, as demonstrated by the XRD (Figure 2(a)) and FT-IR (Figure 2(b)) spectra at different time intervals.

Meanwhile, appropriate reaction temperature was critical for the formation of hierarchical PbS microstars (Figure 4), while other conditions were kept unchanged. As illustrated in Figure 4(a), the products have obvious agglomeration, but no specific morphology when the temperature is 140°C. Increasing the temperature to 160°C yields a mixture of many immature hierarchical PbS microstars with multidendritic arms (Figure 4(b)). As confirmed by the XRD analysis, the products contain some impurities when the temperature is below 180°C (Figure 2(c), curves a-b), owing to the existence of the Pb^{2+}-diphenylthiocarbazone complexes at lower temperature. On the other hand, when the temperature is over 180°C (e.g., 200°C, Figure 4(c); 220°C, Figure 4(d)), the products contain several immature hierarchical PbS microstars with smaller size, where the lobules as building units are transformed to rod-like structures in the products. The smaller sizes of the product can be explained by Ostwald ripening process [35]. The XRD measurements show high purity and single phase when the temperature exceeds 180°C (Figure 2(c), curves c-d).

The control experiments associated with the molar ratios of Pb(II) to diphenylthiocarbazone found that well-defined microstars were obtained only at the appropriate ratio of 1 : 1, while other conditions were kept constant. Specifically, changing the ratio to 1 : 2 produces many single dendrites with the length of ca. 4 μm, as well as several hierarchical PbS microstars left. Besides, the lobules are transformed to rod-like structures with the diameter of 200 nm (Figure 5(a)). In contrast, the products are mainly hierarchical PbS microstars when the ratio is 2 : 1, while the distance is enlarged between the two groups of the symmetric PbS lobules (Figure 5(b)). It means that the ratio of Pb(II) to diphenylthiocarbazone is very important for the morphology of PbS products. This is ascribed to the fact that diphenylthiocarbazone is the sulfur source and also serves as a complex agent for the formation of Pb^{2+}-diphenylthiocarbazone complex.

Meanwhile, there is no product obtained by using water instead of EDA as a solvent, owing to the insolubility of diphenylthiocarbazone in water. Using the mixed solvent with the volume ratio of EDA to water of 1 : 5, the products have obvious agglomeration, and no specific morphology was observed (Figure 6(a)). When the ratio is 1 : 1, the products include many single dendrites (Figure 6(b)), and a large number of immature hierarchical PbS microstars emerged as the ratio is 5 : 1 (Figure 6(c)). These results indicate that EDA as the solvent has critical effects on the shapes of the products.

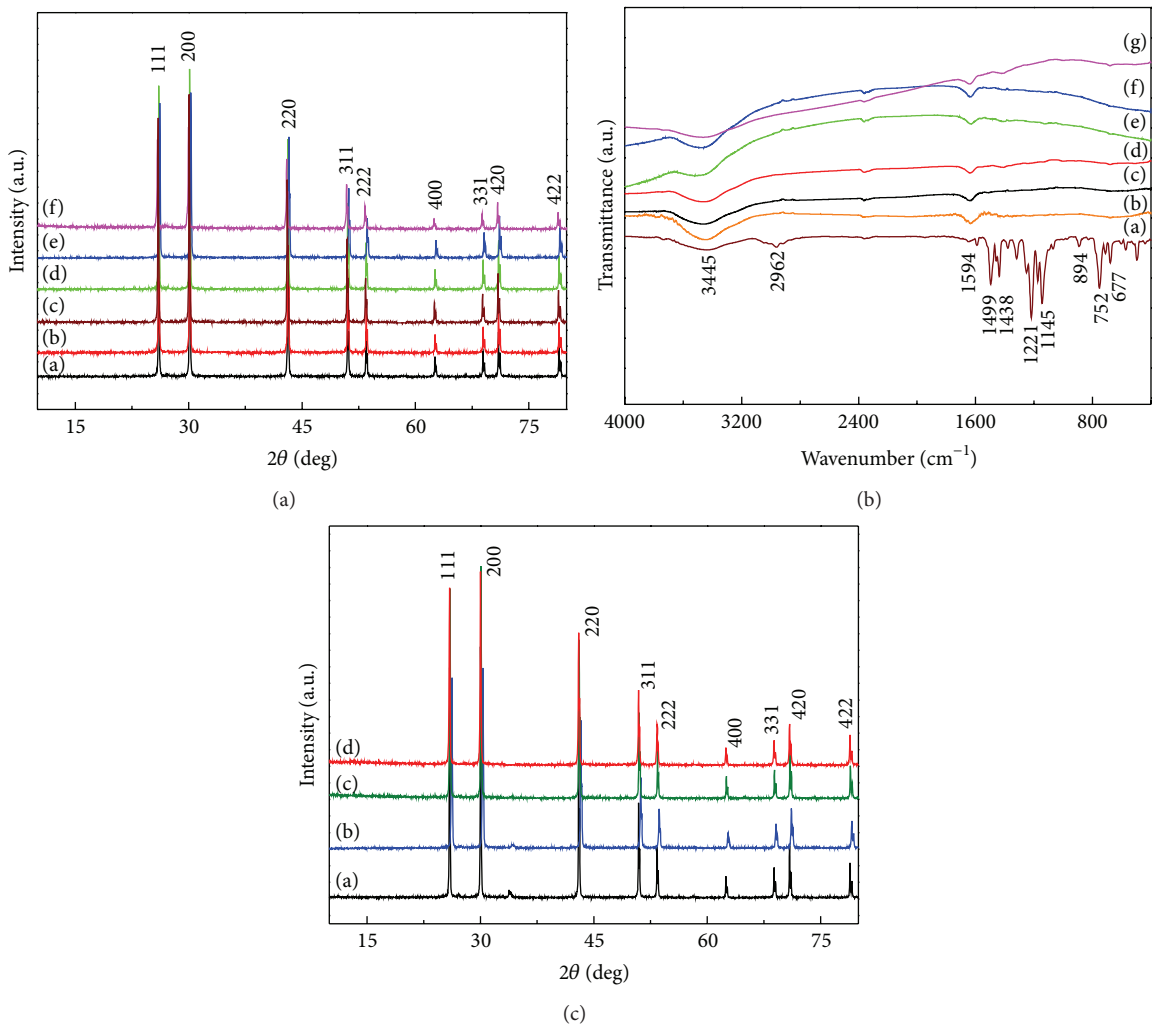

Figure 2: (a) XRD patterns of PbS samples with different reaction time: 0.5 h (curve a), 1 h (curve b), 2 h (curve c), 4 h (curve d), 8 h (curve e), and 16 h (curve f). (b) FT-IR spectra of pure diphenylthiocarbazone (a) and PbS samples taken out at different time intervals: 0.5 h (curve b), 1 h (curve c), 2 h (curve d), 4 h (curve e), 8 h (curve f), and 16 h (curve g). (c) XRD patterns of PbS samples prepared at different reaction temperature: 140°C (curve a), 160°C (curve b), 200°C (curve c), and 220°C (curve d).

Similarly, by replacing EDA with EA as the solvent, the products have no obvious morphology (Figure 7(a)), and there are a few single dendrites with many rod-like structures as subunits when the volume ratio of EDA to EA is 1 : 1 (Figure 7(b)). By increasing the ratio to 2 : 1, many single dendrites are formed, including three groups of layered and symmetrical nanorods (Figure 7(c)). As the ratio is 5 : 1, the products contain many immature multidendritic arms assembled PbS microstars (Figure 7(d)). These results indicate that the morphologies of PbS crystals can be controlled by altering the solvent, where EDA plays an important role in shaping these crystals in the products.

3.2. Growth Mechanism. Generally, the growth mechanism contains an original nucleating stage and a follow-up crystal growth process [36, 37]. The initial nucleation will minimize the system energy, while the subsequent crystal growth would strongly determine the final shapes of the crystals by controlling kinetic and/or thermodynamic parameters [14]. As known, EDA molecules contain two $-NH_2$ groups, which can coordinate with cations, and thereby facilitates the growth of the crystals with desired morphologies [1, 38]. Meanwhile, EDA can influence the epitaxial growth, which can firstly incorporate into the inorganic skeleton and then escape to form crystals with desired shapes [38–41].

In the present reaction system, the possible formation mechanism of hierarchical PbS microstars can be described as a process of rapid nucleation, epitaxial growth, and crystal orientation (Figure 8). Diphenylthiocarbazone contains =S, –NH, –N–N–, –N=N–, and benzene ring, but only =S can interact with Pb^{2+} to form the complex. At the very early stage, the complexes of Pb^{2+}-diphenylthiocarbazone are formed, which are unstable with the increase of the temperature, in comparison with the complexes of Pb^{2+}-EDA. Therefore, the S–C bond in diphenylthiocarbazone is easily ruptured during the solvothermal process, owing to high

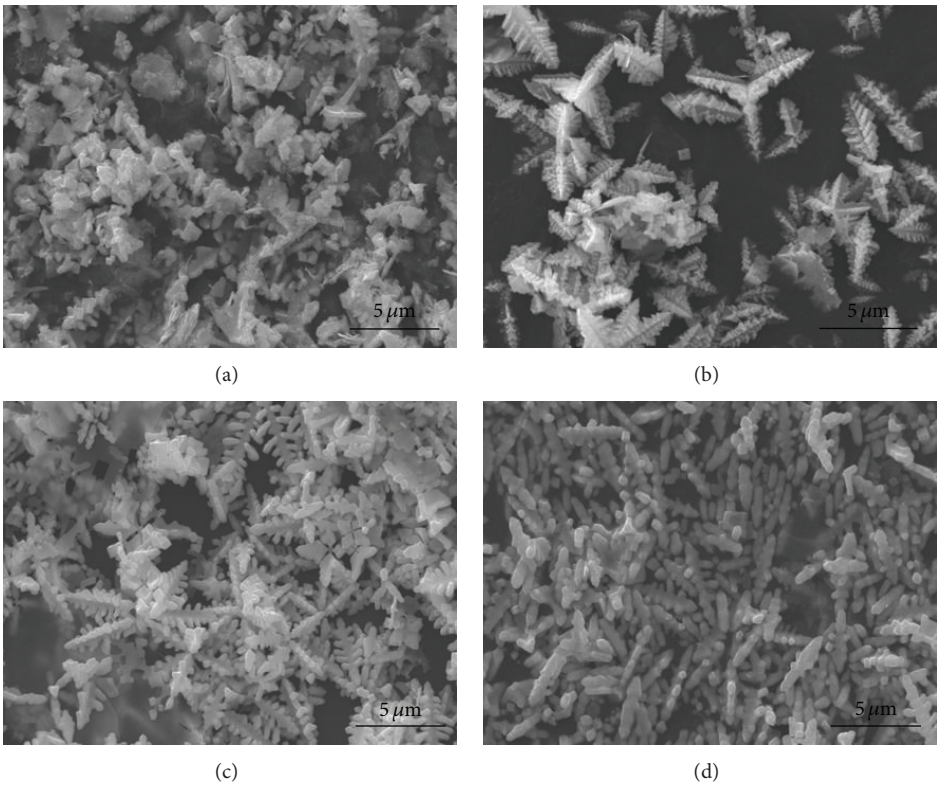

Figure 3: SEM images of the products obtained with different reaction time: 0.5 h (a), 1 h (b), 8 h (c), and 16 h (d).

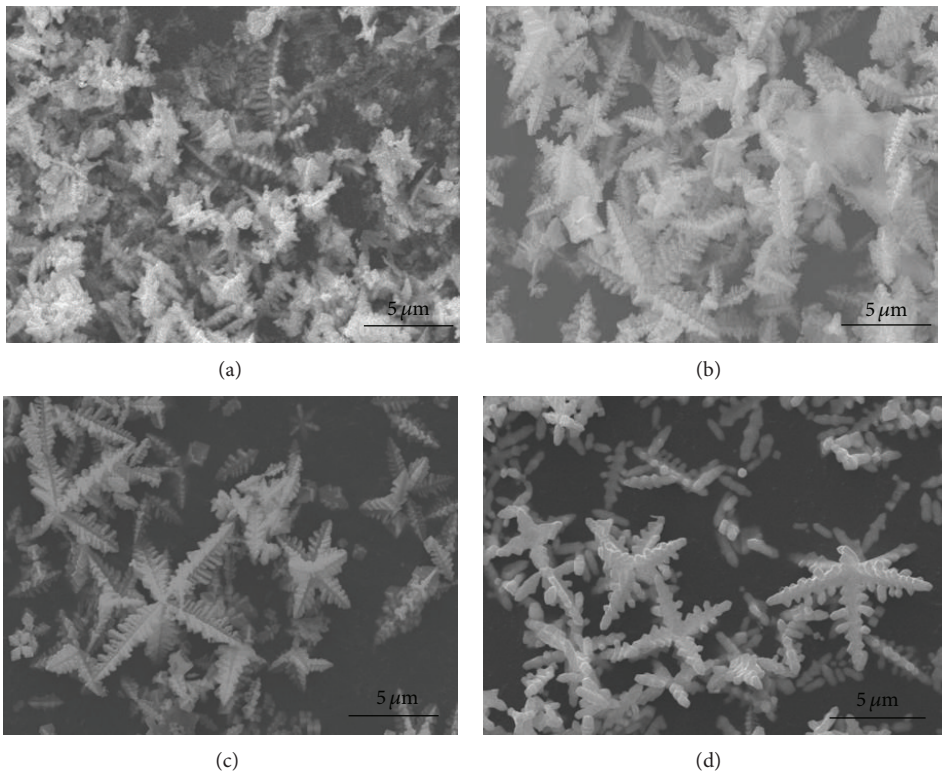

Figure 4: SEM images of the products obtained at different reaction temperature: 140°C (a), 160°C (b), 200°C (c), and 220°C (d).

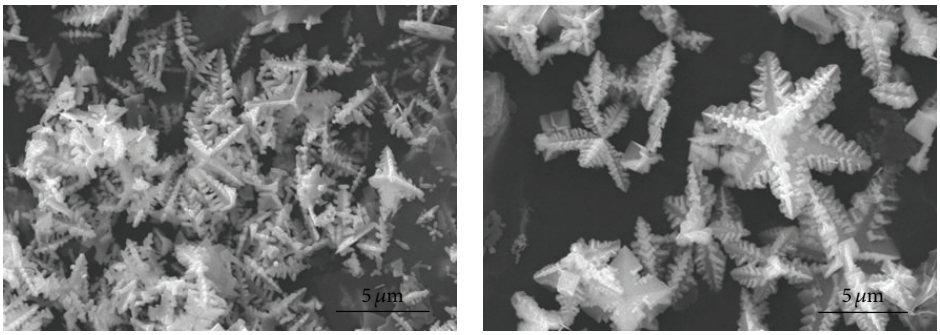

(a) (b)

Figure 5: SEM images of the products prepared with different molar ratios of Pb^{2+} to diphenylthiocarbazone: 1 : 2 (a) and 2 : 1 (b).

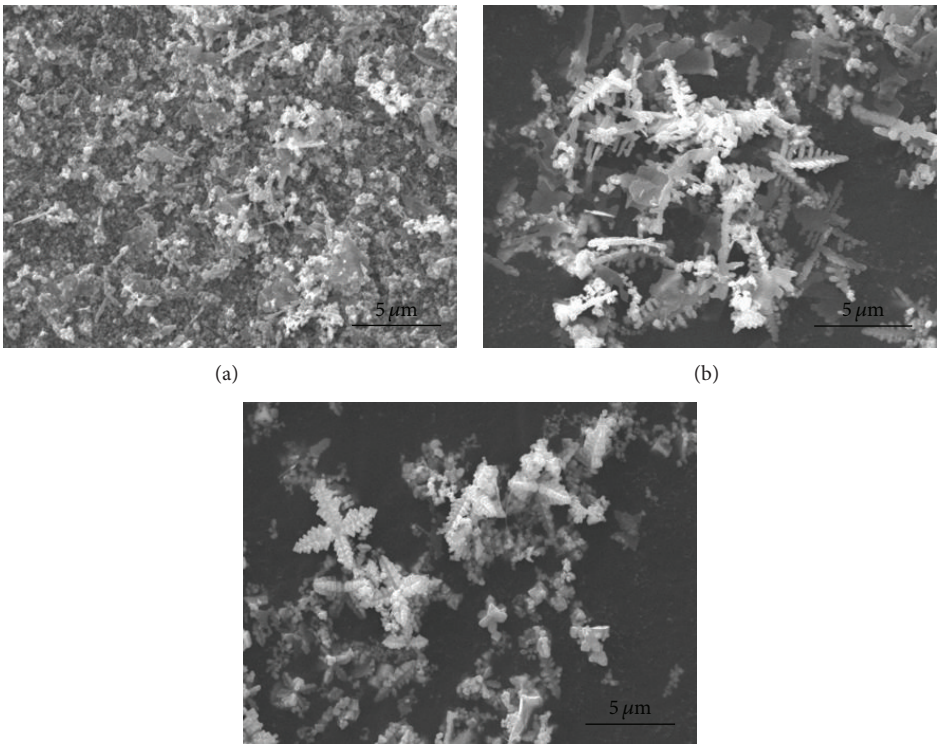

(a) (b)

(c)

Figure 6: SEM images of the samples prepared with different volume ratios of EDA to water: 1 : 5 (a), 1 : 1 (b), and 5 : 1 (c).

temperature and pressure, causing the formation of PbS nuclei. The adjacent EDA molecules are readily covered on the surface of newly generated PbS crystals which serve as building unit for the formation of hierarchical PbS microstars with multidendritic arms via highly epitaxial crystal growth [38–41]. This assumption is confirmed by the control experiments regarding the mixed solvents with various components and also agrees well with the growth of CdS nanorods in the literature [38, 42].

3.3. Optical Property. It is very significant to control the band edge gaps of advanced semiconductors for their practical and potential applications [16]. Figure 9 shows the room-temperature photoluminescence (PL) spectrum of hierarchical PbS microstars with multidendritic arms. A sharp and strong peak is detected at 437 nm with an excitation wavelength of 360 nm, using the excitation slit width and emission slit width of 5 nm. This peak is usually associated with the transition of electrons from the conduction band edges to holes, trapped at the interstitial Pb^{2+} sites [16, 23]. The emission spectra are almost independent on the excitation wavelengths [43], and similar spectra are obtained in each case, albeit with different peak intensities under the identical conditions (data not shown), as reported in the literature [2, 4]. Similar results are obtained for hierarchical

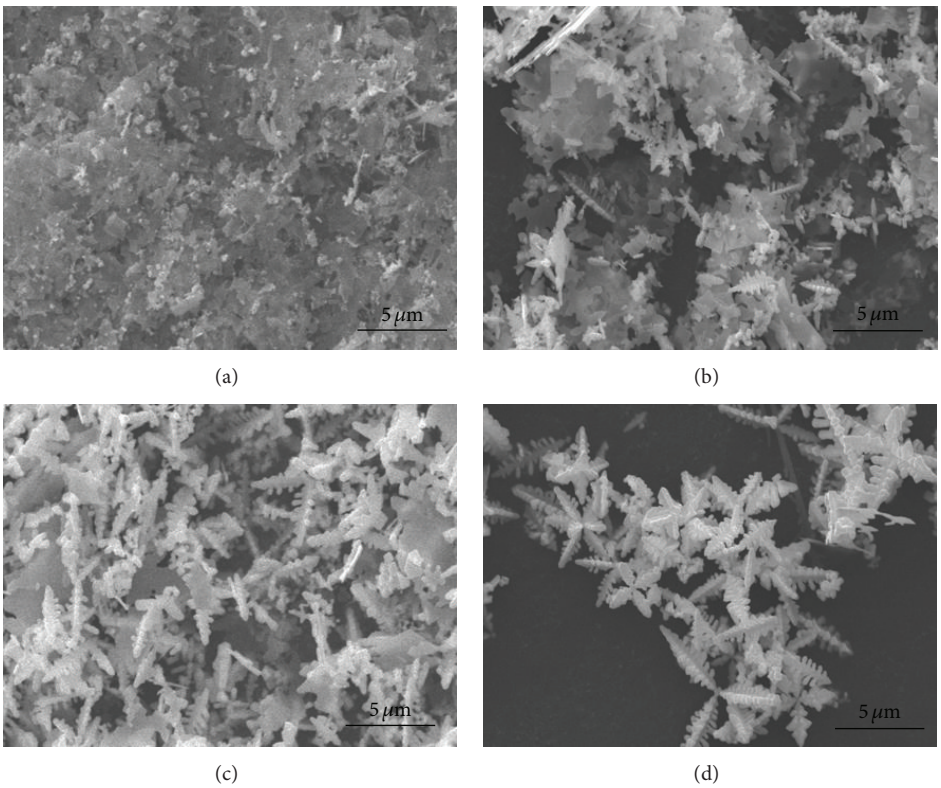

Figure 7: SEM images of the samples prepared at different volume ratios of EDA to EA: 0 : 1 (a), 1 : 1 (b), 2 : 1 (c), and 5 : 1 (d).

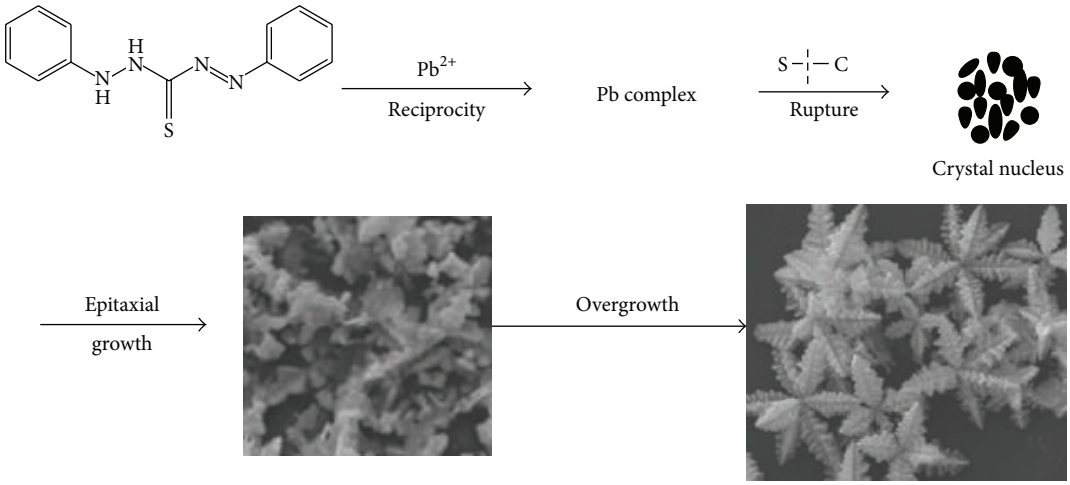

Figure 8: The possible formation mechanism of PbS microstars with multidendritic arms.

PbS microstars [16], as well as PbS nanostructures with a variety of morphologies [23].

4. Conclusions

In summary, a simple and facile method was developed for the solvothermal synthesis of hierarchical PbS microstars with multidendritic arms. Their formation mechanism was discussed based on the control experiments regarding the molar ratios of the precursors, reaction time and temperature, and mixed solvents with different compositions. With an excitation wavelength of 360 nm, a PL peak was detected at 437 nm in the PL spectrum, proving that the as-prepared PbS crystals have potential and practical applications in photoluminescence, photovoltaics, IR photodetectors, electroluminescence, and solar absorbers. This method may provide an effective route to the morphology-controlled synthesis of other hierarchical-structured metal chalcogenides.

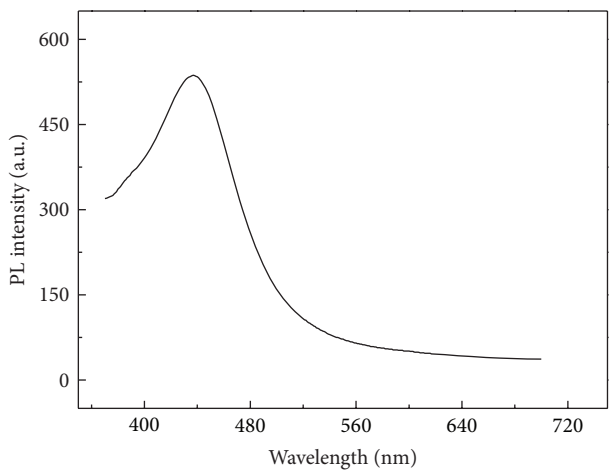

Figure 9: Room-temperature photoluminescence spectrum of PbS microstars with multidendritic arms.

Conflict of Interests

The authors declare that there is no conflict of interests regarding the publication of this paper.

Acknowledgment

This work has been financially supported by the National Natural Science Foundation of China (no. 21275130).

References

[1] Z. Zhang, S. H. Lee, J. J. Vittal, and W. S. Chin, "A simple way to prepare PbS nanocrystals with morphology tuning at room temperature," *Journal of Physical Chemistry B*, vol. 110, no. 13, pp. 6649–6654, 2006.

[2] P. Zhao, J. Wang, G. Cheng, and K. Huang, "Fabrication of symmetric hierarchical hollow PbS microcrystals via a facile solvothermal process," *The Journal of Physical Chemistry B*, vol. 110, no. 45, pp. 22400–22406, 2006.

[3] M. S. Bakshi, P. Thakur, S. Sachar et al., "Aqueous phase surfactant selective shape controlled synthesis of lead sulfide nanocrystals," *The Journal of Physical Chemistry C*, vol. 111, no. 49, pp. 18087–18098, 2007.

[4] G. Zhou, M. Lü, Z. Xiu, S. Wang, H. Zhang, and Y. Zhou, "Controlled synthesis of high-quality PbS star-shaped dendrites, multipods, truncated nanocubes, and nanocubes and their shape evolution process," *The Journal of Physical Chemistry B*, vol. 110, no. 13, pp. 6543–6548, 2006.

[5] Y. K. Mishra, S. Kaps, A. Schuchardt et al., "Versatile fabrication of complex shaped metal oxide nano-microstructures and their interconnected networks for multifunctional applications," *KONA Powder and Particle Journal*, vol. 31, no. 1, pp. 92–110, 2014.

[6] X. Jin, M. Götz, S. Wille, Y. K. Mishra, R. Adelung, and C. Zollfrank, "A novel concept for self-reporting materials: stress sensitive photoluminescence in ZnO tetrapod filled elastomers," *Advanced Materials*, vol. 25, no. 9, pp. 1342–1347, 2013.

[7] O. Lupan, V. Cretu, M. Deng et al., "Versatile growth of free-standing orthorhombic α-molybdenum trioxide nano- and microstructures by rapid thermal processing for gas nanosensors," *The Journal of Physical Chemistry C*, vol. 118, no. 27, pp. 15068–15078, 2014.

[8] Y. K. Mishra, S. Kaps, A. Schuchardt et al., "Fabrication of macroscopically flexible and highly porous 3D semiconductor networks from interpenetrating nanostructures by a simple flame transport approach," *Particle & Particle Systems Characterization*, vol. 30, no. 9, pp. 775–783, 2013.

[9] T. Reimer, I. Paulowicz, R. Röder et al., "Single step integration of ZnO Nano-and microneedles in Si trenches by novel flame transport approach: whispering gallery modes and photocatalytic properties," *ACS Applied Materials and Interfaces*, vol. 6, no. 10, pp. 7806–7815, 2014.

[10] S. Chen, L. A. Truax, and J. M. Sommers, "Alkanethiolate-protected PbS nanoclusters: synthesis, spectroscopic and electrochemical studies," *Chemistry of Materials*, vol. 12, no. 12, pp. 3864–3870, 2000.

[11] K.-T. Yong, Y. Sahoo, K. R. Choudhury, M. T. Swihart, J. R. Minter, and P. N. Prasad, "Control of the morphology and size of PbS nanowires using gold nanoparticles," *Chemistry of Materials*, vol. 18, no. 25, pp. 5965–5972, 2006.

[12] T. Huang, Q. Zhao, J. Xiao, and L. Qi, "Controllable self-assembly of pbs nanostars into ordered structures: close-packed arrays and patterned arrays," *ACS Nano*, vol. 4, no. 8, pp. 4707–4716, 2010.

[13] Y. Yang, J. Li, H. Wu, E. Oh, and D. Yu, "Controlled ambipolar doping and gate voltage dependent carrier diffusion length in lead sulfide nanowires," *Nano Letters*, vol. 12, no. 11, pp. 5890–5896, 2012.

[14] X. Duan, J. Ma, Y. Shen, and W. Zheng, "A novel PbS hierarchical superstructure guided by the balance between thermodynamic and kinetic control via a single-source precursor route," *Inorganic Chemistry*, vol. 51, no. 2, pp. 914–919, 2012.

[15] H. Zeng, Z. A. Schelly, K. Ueno-Noto, and D. S. Marynick, "Density functional study of the structures of lead sulfide clusters (PbS) n ($n = 1$–9)," *The Journal of Physical Chemistry A*, vol. 109, no. 8, pp. 1616–1620, 2005.

[16] A.-J. Wang, Q.-C. Liao, J.-J. Feng, P.-P. Zhang, Z.-M. Zhang, and J.-R. Chen, "D-penicillamine-assisted self-assembly of hierarchical PbS microstars with octa-symmetric-dendritic arms," *Crystal Growth and Design*, vol. 12, no. 2, pp. 832–841, 2012.

[17] C. Li, Y. Zhao, F. Li, Z. Shi, and S. Feng, "Near-infrared absorption of monodisperse water-soluble PbS colloidal nanocrystal clusters," *Chemistry of Materials*, vol. 22, no. 5, pp. 1901–1907, 2010.

[18] H. Cao, Q. Gong, X. Qian, H. Wang, J. Zai, and Z. Zhu, "Synthesis of 3-D hierarchical dendrites of lead chalcogenides in large scale via microwave-assistant method," *Crystal Growth & Design*, vol. 7, no. 2, pp. 425–429, 2007.

[19] Y. Hou, H. Kondoh, and T. Ohta, "PbS cubes with pyramidal pits: an example of etching growth," *Crystal Growth & Design*, vol. 9, no. 7, pp. 3119–3123, 2009.

[20] M. Bashouti and E. Lifshitz, "PbS sub-micrometer structures with anisotropic shape: ribbons, wires, octapods, and hollowed cubes," *Inorganic Chemistry*, vol. 47, no. 2, pp. 678–682, 2008.

[21] S. F. Wang, F. Gu, and M. K. Lü, "Sonochemical synthesis of hollow PbS nanospheres," *Langmuir*, vol. 22, no. 1, pp. 398–401, 2006.

[22] G. Q. Xin, H. P. Ding, Y. G. Yang et al., "Triangular single-crystalline nanorings of PbS formed at the air/water interface," *Crystal Growth & Design*, vol. 9, no. 4, pp. 2008–2012, 2009.

[23] S. Xiong, B. Xi, D. Xu et al., "L-cysteine-assisted tunable synthesis of PbS of various morphologies," *The Journal of Physical Chemistry C*, vol. 111, no. 45, pp. 16761–16767, 2007.

[24] Y. Ma, L. Qi, J. Ma, and H. Cheng, "Hierarchical, star-shaped PbS crystals formed by a simple solution route," *Crystal Growth & Design*, vol. 4, no. 2, pp. 351–354, 2004.

[25] T. Mandal, G. Piburn, V. Stavila et al., "New mixed ligand single-source precursors for PbS nanoparticles and their solvothermal decomposition to anisotropic nano- and microstructures," *Chemistry of Materials*, vol. 23, no. 18, pp. 4158–4169, 2011.

[26] P. L. Nichols, M. Sun, and C. Z. Ning, "Influence of supersaturation and spontaneous catalyst formation on the growth of PbS wires: toward a unified understanding of growth modes," *ACS Nano*, vol. 5, no. 11, pp. 8730–8738, 2011.

[27] J. Xiang, H. Cao, Q. Wu, S. Zhang, and X. Zhang, "L-cysteine-assisted self-assembly of complex PbS structures," *Crystal Growth and Design*, vol. 8, no. 11, pp. 3935–3940, 2008.

[28] M. A. Hines and G. D. Scholes, "Colloidal PbS nanocrystals with size-tunable near-infrared emission: observation of post-synthesis self-narrowing of the particle size distribution," *Advanced Materials*, vol. 15, no. 21, pp. 1844–1849, 2003.

[29] J. Joo, H. B. Na, T. Yu et al., "Generalized and facile synthesis of semiconducting metal sulfide nanocrystals," *Journal of the American Chemical Society*, vol. 125, no. 36, pp. 11100–11105, 2003.

[30] Y. Ni, H. Liu, F. Wang et al., "Shape controllable preparation of PbS crystals by a simple aqueous phase route," *Crystal Growth & Design*, vol. 4, no. 4, pp. 759–764, 2004.

[31] N. Wang, X. Cao, L. Guo, S. Yang, and Z. Wu, "Facile synthesis of PbS truncated octahedron crystals with high symmetry and their large-scale assembly into regular patterns by a simple solution route," *ACS Nano*, vol. 2, no. 2, pp. 184–190, 2008.

[32] Z. Zeng, S. Wang, and S. Yang, "Synthesis and characterization of PbS nanocrystallites in random copolymer ionomers," *Chemistry of Materials*, vol. 11, no. 11, pp. 3365–3369, 1999.

[33] J. Zhou, G. Zhao, J. Yang, and G. Han, "Diphenylthiocarbazone (dithizone)-assisted solvothermal synthesis and optical properties of one-dimensional CdS nanostructures," *Journal of Alloys and Compounds*, vol. 509, no. 23, pp. 6731–6735, 2011.

[34] S.-S. Li, J.-N. Zheng, X. Ma et al., "Facile synthesis of hierarchical dendritic PtPd nanogarlands supported on reduced graphene oxide with enhanced electrocatalytic properties," *Nanoscale*, vol. 6, no. 11, pp. 5708–5713, 2014.

[35] C. C. Yec and H. C. Zeng, "Synthesis of complex nanomaterials via Ostwald ripening," *Journal of Materials Chemistry A*, vol. 2, no. 14, pp. 4843–4851, 2014.

[36] S. Mann, "Synthese von bariumsulfat-spiralen aus tensid-beschichteten nanopartikeln," *Angewandte Chemie*, vol. 112, no. 19, pp. 3532–3548, 2000.

[37] M. J. Siegfried and K.-S. Choi, "Directing the architecture of cuprous oxide crystals during electrochemical growth," *Angewandte Chemie*, vol. 117, no. 21, pp. 3282–3287, 2005.

[38] P. Zhao and K. Huang, "Preparation and characterization of netted sphere-like CdS nanostructures," *Crystal Growth & Design*, vol. 8, no. 2, pp. 717–722, 2008.

[39] X. Wang and Y. Li, "Solution-based synthetic strategies for 1-D nanostructures," *Inorganic Chemistry*, vol. 45, no. 19, pp. 7522–7534, 2006.

[40] A.-J. Wang, F.-F. Li, Z. Bai, and J.-J. Feng, "Large-scale electrosynthesis of Pd nanodendrites and their improved electrocatalytic properties for methanol oxidation," *Electrochimica Acta*, vol. 85, pp. 685–692, 2012.

[41] J.-J. Feng, A.-Q. Li, Z. Lei, and A.-J. Wang, "Low-potential synthesis of 'clean' Au nanodendrites and their high performance toward ethanol oxidation," *ACS Applied Materials & Interfaces*, vol. 4, no. 5, pp. 2570–2576, 2012.

[42] J. Yang, J.-H. Zeng, S.-H. Yu, L. Yang, G.-E. Zhou, and Y.-T. Qian, "Formation process of CdS nanorods via solvothermal route," *Chemistry of Materials*, vol. 12, no. 11, pp. 3259–3263, 2000.

[43] H. Cao, G. Wang, S. Zhang, and X. Zhang, "Growth and photoluminescence properties of PbS nanocubes," *Nanotechnology*, vol. 17, no. 13, pp. 3280–3287, 2006.